Prediction of Stacking Faults in β-Silicon Carbide: X-ray and NMR Studies

Hiroshi Tateyama,* Hiroaki Noma, Yoshio Adachi, and Masahiro Komatsu

Kyushu National Industrial Research Institute, Shuku-machi, Tosu-shi, Saga Prefecture, Japan 841

Received September 11, 1996. Revised Manuscript Received November 21, 1996[⊗]

The X-ray powder diffraction profiles of SiC were calculated on the basis of the matrix intensity equation method in order to investigate the stacking sequence in β-SiC powders. In the case of "reichweite" $R = 4$, where R represents the correlation distance over which the occurrence of a layer type affects the probability of occurrence of a given layer, the structural relationship of the stacking sequence among 2H, 3C, 4H, and 6H polytypes can be discussed. High-resolution solid-state nuclear magnetic resonance (NMR) spectroscopy has been used to obtain the information concerning the different kinds of sites in 2H, 3C, 4H, and 6H polytypes. This approach reveals that it is possible to determine the amounts of stacking faults and the kinds of stacking modes in SiC by comparing the calculated X-ray powder diffraction profiles and by the simulation of each deconvoluted signal in the NMR spectra. The calculated result indicates that all of the β-SiC samples used consist of mainly the 3C type and some amount of the 6H type stacking modes.

Introduction

The properties of ultrafine particles of SiC are of current interest because of the use of SiC in high-performance ceramic composites,[1] the preparation of SiC thin films in microelectronic and semiconductor systems,[2] and the capability of tailoring electric and optical properties for optoelectronic applications.[3] All forms of silicon carbide are based on the diamond structure, with both silicon and carbon tetrahedral and with alternating silicon and carbon layers. The polytypic modifications are the cubic zinc blend type of β-SiC expressed as 3C by Ramsdell notation[4,5] and the hexagonal wurzite type of α-SiC expressed as 2H, 4H, 6H, and 15R by Ramsdell notation. In addition to short- and long-period polytypes of SiC, stacking faults also exist in the structure between each SiC_4 (or CSi_4) layer. The stacking faults are commonly included in the submicron SiC powders obtained by heat treatments of soot-like mixed powders of silicon dioxide and carbon,[6] plasma treatments of SiH_4 and Cl_4 gases,[7,8] or chemical vapor deposition methods.[9] These synthetic commercial SiC powders have been assigned to be β-SiC including a small amount of α-SiC as impurities. However, it is usually difficult to determine the amount of stacking faults quantitatively using the X-ray powder diffraction method.

The intensity of X-rays scattered from close-packed structures containing random or nonrandom distribution of stacking faults can be calculated either by the use of difference equations[10,11] or by means of matrix intensity equations.[12−14] Recently the analytical method of stacking faults in the structure of SiC has been proposed quantitatively on the basis of the matrix intensity equation method.[6] In a previous report,[6] the "reichweite" R defined by Jagodzinski[15] was restricted to $R = 2$. Therefore, the stacking faults in SiC were discussed only among 2H and 3C polytypes. However, the structural relationship of the stacking faults among 2H, 3C, 4H, and 6H polytypes can be discussed using an order of R higher than 4.

During the past few years, the polytypes of SiC have been studied by solid-state ^{29}Si and ^{13}C NMR.[16−29] The NMR studies of SiC have provided an explanation of

⊗ Abstract published in *Advance ACS Abstracts,* January 15, 1997.

(1) Kim, Y. K.; Mitomo, M.; Hirotsuru, H. *J. Am. Ceram. Soc.* **1995**, *78*, 3145.
(2) Morkoc, H.; Strite, S.; Gao, G. B.; Lin, M. E.; Sverdlov, B.; Burns, M. *J. Appl. Phys.* **1994**, *76*, 1363.
(3) Hattori, Y.; Kruangam, D.; Toyama, T.; Okamoto, H.; Hamakawa, Y. *J. Non-Cryst. Solids* **1987**, *97*, 1079.
(4) Ramsdell, L. S. *Am. Mineral.* **1944**, *29*, 431.
(5) Ramsdell, L. S.; Kohn, J. A. *Acta Crystallogr.* **1952**, *5*, 215.
(6) Tateyama, H.; Sutoh, N.; Murakawa, N. *J. Ceram. Soc. Jpn., Int. Ed.* **1988**, *96*, 1003.
(7) Hollabaugh, C. M.; Hull, D. E.; Newkirk, L. R.; Petrovic, J. J. *Mater. Sci.* **1983**, *18*, 3190.
(8) Yoshida, T.; Tani, T.; Nishimura, T.; Asahi, T. *J. Appl. Phys.* **1983**, *54*, 640.
(9) Sadakata, M.; Baba, H.; Sato, M.; Sakai, T. *Kagaku Kougyou Ronbunshi* **1989**, *15*, 91.
(10) Patterson, M. S. *J. Appl. Phys.* **1952**, *23*, 805.
(11) Willson, A. J. C. *X-ray optics*; John Wiley & Sons: New York, 1949; pp 55−96.
(12) Hendricks, S.; Teller, E. *J. Chem. Phys.* **1942**, *10*, 147.
(13) Kakinoki, J.; Komura, Y. *J. Phys. Soc. Jpn.* **1954**, *9*, 169.
(14) Kakinoki, J. *Acta Crystallogr.* **1967**, *23*, 875.
(15) Jadgozinski, H. *Acta Crystallogr.* **1949**, *2*, 201.
(16) Finalay, G. R.; Hartman, J. S.; Richardson, M. F.; Williams, B. L. *J. Chem. Soc., Chem. Commun.* **1985**, 159.
(17) Inkrott, K. E.; Wharry, S. M.; O'Donnell, D. J. *Mater. Res. Soc. Symp. Proc.* **1986**, *73*, 165.
(18) Hartman, J. S.; Richardson, M. F.; Scherriff, B. L.; Winsborrow, B. G. *J. Am. Chem. Soc.* **1987**, *109*, 6059.
(19) Guth, J. R.; Petuskey, W. T. *J. Phys. Chem.* **1987**, *81*, 5361.
(20) Carduner, K. R.; Carter III, R. O.; Rokosz, M. J.; Peters, C.; Crosbie, G. M.; Stiles, E. D. *Anal. Chem.* **1987**, *59*, 2794.
(21) Carduner, K. R.; Carter III, R. O. *Ceram. Int.* **1989**, *15*, 327.
(22) Wagner, G. W.; Na, B. K.; Vannice, M. A. *J. Phys. Chem.* **1989**, *93*, 5061.
(23) Carduner, K. R.; Shinozaki, S. S.; Rokosz, M. J.; Peters, C.; Whalen, T. *J. Am. Ceram. Soc.* **1990**, *73*, 2281.
(24) Dando, N.; Tadayyoni, M. A. *J. Am. Ceram. Soc.* **1990**, *73*, 2242.
(25) Apperley, D.; Harris, R.; Marshall, G. L.; Thompson, D. *J. Am. Ceram. Soc.* **1991**, *74*, 777.
(26) Richardson, M. F.; Hartman, J. S.; Guo, D.; Winsborrow, B. *Chem. Mater.* **1992**, *4*, 318.
(27) Guo, D.; Hartman, J. S.; Richardson, M. F. *Can. J. Chem.* **1992**, *70*, 700.
(28) Tougne, P.; Hommel, H.; Legrand, A. P.; Cauchetier, M.; Luce, M. *Diamond Relat. Mater.* **1992**, *1*, 360.

S0897-4756(96)00471-1 CCC: $14.00 © 1997 American Chemical Society

the chemical shift differences between different polytypes, which indicates that the chemical shifts demonstrate sensitivity to longer range variation in crystal structure. In NMR spectra, the polytypes can be described using four different combinations (A–D). For example, the 3C polytype contains only the A-type environment, the 4H contains equal numbers of B- and C-type environments, the 6H contains equal numbers of A-, B-, and C-type environments, and the 2H is composed entirely of the D-type environment.[18] If the concept of "sphere of influence" in NMR can be applied to one of the "reichweite" in X-ray diffraction, the prediction of the stacking faults and stacking sequence in SiC can be made using calculated X-ray powder diffraction profiles and by the simulation of each deconvoluted signal in the NMR spectra.

Experimental Section

General Comments. The synthesis of SiC was followed by the method described in a previous paper.[6] A liquid mixture of $SiCl_4$ or CH_3SiCl_3 and a petroleum distillate was spray-pyrolyzed in a propane flame at temperature ranging from 1000 and 1200 °C. The produced mixed powder of carbon and silicon dioxide was collected by a bag filter. The specific surface area of the mixed powder was 37.4 m^2/g, and the weight ratio of carbon to silicon dioxide was 1.6. The powdered mixture of carbon and silicon dioxide was compressed and heated in a graphite crucible for 30 min at 1700, 1800, 1900, and 2000 °C in a nitrogen atmosphere using an rf furnace. The specimens heated at these temperatures are designated here as S-17, S-18, S-19, and S-20, respectively. Residual carbon included in these specimens was burned out for 20 h at 700 °C in air. The silicon dioxide residue was removed with hydrofluoric acid. Plasma-synthesized β-SiC (produced by Sumitomo Osaka Cement Co., Ltd.) was also used to compare with the structural properties of the present sample. This sample (P-10) includes graphite as an impurity. The specific surface area and the averaged particle size were 48 cm^3/g and 0.03 μm, respectively.

X-ray powder diffraction measurements of SiC powders were performed by step scan technique using a Philips diffractometer (APD15). The measuring conditions were as follows: step width, 0.05; measuring time of each step, 40 s. The ^{29}Si spectra of SiC powders were obtained under conditions of magic-angle spinning (MAS) at ambient temperature using a Bruker AC200 spectrometer with a Bruker MAS probe tuned to silicon at a frequency of 39.765 MHz. The samples were packed into zirconia double air-bearing rotors which required 0.5 g of powder, and the sample spinning rates were 3.3 kHz. The ^{29}Si spectrum was obtained after 128 pulses using 45° pulse, 1800 s pulse delays, and 10 Hz line broadening.

Calculation Procedure. The calculations of X-ray powder diffraction profiles of SiC with stacking faults are based on the one-dimensional stacking faults ranging from a hexagonal close-packing modification to a cubic close-packing modification described in a previous paper.[6] The intensity equation of the X-ray diffraction in a matrix form is given first as follows:[13]

$$I = N\,\mathrm{spur}\,VF + (N - m)\,\mathrm{spur}\,VFP^m \exp(-2\pi i m\zeta) + \text{conjugate} \quad (1)$$

where N is the total number of the layers, V is the matrix of the layer form factor; F is the matrix of the existing probability, m is the number of layers at the arbitrary point, P is the matrix of the continuing probability of the layer to the next layer, and ζ is the continuous coordinate along c^* in the reciprocal space. The order of the matrixes in eq 1 can be reduced to $^1/_3$ by mathematical reduction.[14] The intensity, $I(\xi,\eta,\zeta)$, of the diffuse scattering from a one-dimensionally disordered crystal is expressed by[30,31]

$$I(\xi,\eta,\zeta) = NL(\xi\eta)\, X(\zeta) \quad (2)$$

where $L(\xi\eta)$ is the Laue function along a^* and b^*, and $X(\zeta)$ is the intensity distribution along the reciprocal lattice line. The X-ray powder diffraction profile, $I_D(2\theta)$, with stacking faults can be expressed as follows[6] on the basis of eq 2:

$$I_D(2\theta) = \sum nKP(2\theta)\, R(\varphi)\frac{\lambda^2 \Delta l}{16\pi r^2 \sin(\theta)} G_D(2\theta)\, X(\zeta) \quad (3)$$

$$G_D(2\theta) = \int G(\xi\eta)\, dS$$

where $\sum n$ is the total number of the fine particles; K is a constant, $P(2\theta)$ is the polarization factor, $R(\varphi)$ is the preferred orientation factor; φ is the acute angle between the preferred orientation direction and the reciprocal lattice vector, λ is the wavelength, Δl is the small fraction of the distance along the Debye–Scherrer ring, and r is the radius of the Debye–Scherrer ring. $G(\xi\eta)$ is the Gaussian function used in place of the Laue function, and dS is the area fraction perpendicular to the scattering vector. $R(\varphi)$ is fixed at 1, because the present synthetic SiC particles do not have a plate- or rodlike shape.

If there are no stacking faults in the structure, the X-ray powder diffraction profile, $I_P(2\theta)$, is written as follows:[6]

$$I_P(2\theta) = KP(2\theta)\, F(hkl)^2 \frac{R(\varphi)\lambda^3 \Delta V \delta l}{8\pi r v^2 \sin(\theta) \sin(2\theta)} \quad (4)$$

where $F(hkl)$ is the structure factor, hkl represents the indexes of reflection, ΔV is the volume fraction of the sample, v is the volume of the unit cell, and $\Omega(2\theta)$ is the asymmetric modified Lorentzian function,[32] which has the form

$$\Omega(2\theta) = \frac{4\sqrt{\sqrt{2}-1}}{\pi W}\left\{1 + Q\left(\frac{1 + H_4}{H_4}\right)^2 \frac{\sqrt{2}-1}{W^2}(2\theta - 2\theta_{jk})^2\right\}^{-2} \quad (5)$$

where W and H_4 are the half-width and asymmetry parameters, and Q takes a value of 1 or H_4^2 according to $2\theta < 2\theta_{jk}$ or $2\theta > 2\theta_{jk}$. The half-width is given by the formula

$$W = 2(H_1 \tan^2(\theta) + H_2 \tan(\theta) + H_3)^{1/2} \quad (6)$$

where H_1, H_2, and H_3 are half-width parameters. The total powder diffraction profile, $I_T(2\theta)$, can be expressed using eqs 3 and 4 as follows:

$$I_T(2\theta) = I_D(2\theta) + I_P(2\theta) \quad (7)$$

The X-ray powder diffraction profiles of one-dimensionally disordered SiC are calculated on the basis of the three different types of layers using eq 7.

Results and Discussion

Correlations between Calculated XRD Profiles and NMR Spectra. The number R denotes the correlation distance over which the occurrence of a layer type affects the probability of occurrence of a given layer. The designation $R = 1$ means that only adjacent layer types affect the probability of occurrence of a given layer. This describes nearest-neighbor ordering and gives rise, for equal proportions of three components, to an alternating structure. In the hexagonal close-

(29) Tougne, P.; Hommel, H.; Legrand, A. P.; Herlin, N.; Luce, N.; Cauchetier, M. *Diamond Relat. Mater.* **1993**, *2*, 486.

(30) Onoda, M.; Kawada, I. *Acta Crystallogr.* **1980**, *A36*, 134.
(31) Onoda, M.; Saeki, M.; Kawada, I. *Acta Crystallogr.* **1980**, *A36*, 952.
(32) Toraya, H.; Marumo, F. *Rep. Res. Lab. Engin. Mater.* **1980**, *5*, 55.

Table 1. Matrixes of Continuing Probabilities (α Values) with the Chemical Shifts[25] in NMR Spectra

	B C A B cc A-site	A C A B hc C-site	A C A C hh D-site	B C A C ch B-site
A B C A	α_1			$1-\alpha_1$
cc	ccc(3C)			cch(6H)
A-site	−18.4 ppm (A_{3C})			−14.7 ppm (A_{6H})
C B C A	α_2			$1-\alpha_2$
hc	hcc(6H)			hch(4H)
C-site	−25.4 ppm (C_{6H})			−22.5 ppm (C_{4H})
C A C A		α_3	$1-\alpha_3$	
hh		hhc(new)	hhh(2H)	
D-site		X_1 ppm (D_{X1})	−20.0 ppm (D_{2H})	
B A C A		α_4	$1-\alpha_4$	
ch		chc(4H,6H)	chh(new)	
B-site		−20.3 ppm[a] ($B_{4H,6H}$)	X_2 ppm (B_{X2})	

[a] Averaged value of −19.7 ppm (6H) and −20.9 ppm (4H).[25]

packed model, the adjacent silicon layers are 0.252 nm apart. One-half of the correlation distance for $R = 2$, 3, and 4 then becomes 0.252, 0.378, and 0.504 nm, respectively. One-half of the X-ray diffraction correlation distance being 0.504 nm for $R = 4$ therefore nearly corresponds to the radius of the "sphere of influence" being 0.50 nm in the NMR spectra.[18] The number of adjacent layers for $R = 4$ is 4. To describe the stacking sequence of the layers, the ABC notation is used in a closed-packed structure. For a simple β-modification, for example, the second layer of the silicon atom (or of carbon atom) layers is obviously displaced with respect to one chosen as the first layer by ($^1/_3$, $^2/_3$, $^1/_3$) and the third layer by ($^2/_3$, $^1/_3$, $^2/_3$). The fourth layer at (0,0,$^3/_3$) is then directly over the first. The stacking sequence of the layers in these four positions is designated as ABCA. Therefore, the four kinds of stacking sequences for $R = 4$ can be expressed as ABCA, ABAC, ABAB, and ABCB. The Wyckoff sequences[33] are useful for our subsequent discussion of types of silicon (or carbon) environments in different polytypes. His designation H corresponds to a hexagonal-closed packed distribution (ABA), and designation C corresponds to a cubic closed-pack configuration (ABC). In the present report, we use "h" and "c" not to confuse the designations of layer C and C-type used in the NMR spectra. The stacking sequences of ABCA, ABAC, ABAB, and ABCB can be rewritten as cc, hc, hh, and ch, respectively.

The continuing probabilities of four kinds of stacking sequences ($R = 4$) are expressed as α_1, α_2, α_3, and α_4. If, for example, ABCA(cc) is followed by a B layer with a probability α_1, we get ABCAB(ccc), which corresponds to a 3C polytype. On the other hand, if ABCA(cc) is followed by a C layer with a probability $1 - \alpha_1$, we get ABCAC(cch), which corresponds to a 6H polytype. If these two kinds of stacking sequences are compared with the chemical shifts of four kinds of environments in the NMR spectra, the A-site in the NMR spectra can be divided into two groups, 6H and 3C polytypes. The assignment can then be made as follows: the −13.9 to −14.7 ppm[18,19,24,25] and −18.3 to −18.4 ppm signals[18,19,23] correspond to the cch and ccc stacking sequences, respectively. When the ABAC(hc) is followed by a B layer with a probability α_2, the ordering of the layers becomes ABACB(hcc), which corresponds to a 6H polytype. However, if the ABAC(hc) is followed by an A layer with $1 - \alpha_2$, the ordering of the stacking

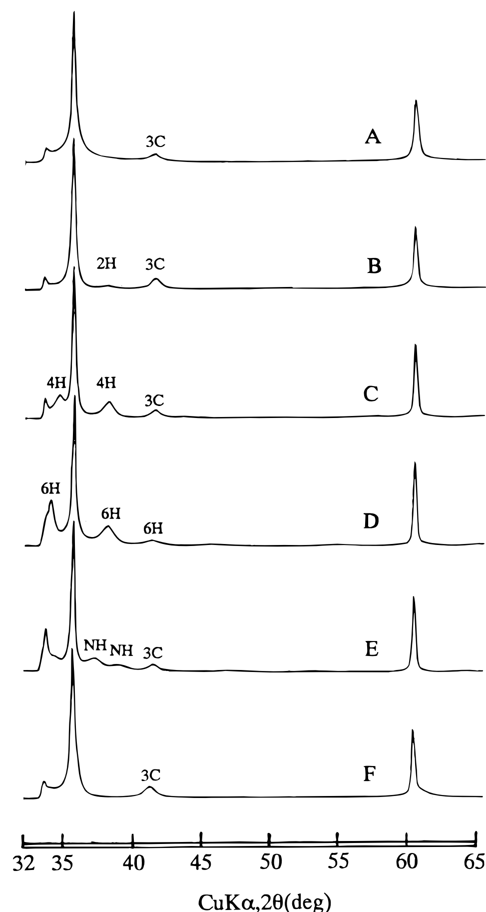

Figure 1. Observed X-ray diffraction pattern (A) and calculated profiles (B−F) using the various α values. NH peak assigned to new stacking sequence (chh and hhc).

sequence becomes ABACA(hch), which is consistent with a 4H polytype. The hcc and hch stacking sequences are assigned to −24.5 to −25.4 ppm[18,19,24,25] in 6H and −22.5 ppm[25] in 4H polytypes, respectively. When ABAB(hh) is followed by an A layer with a probability $1 - \alpha_3$, the stacking sequence becomes ABABA(hhh), corresponding to a 2H polytype. If ABAB(hh) is followed by a C layer with a probability α_3, we get ABABC(hhc). The −20.0 ppm signals[25] in the NMR spectra can be assigned to the hhh sequence; however, none of the other signals can be assigned to the hhc stacking sequence because it does not appear in the usual polytypes (2H, 3C, 4H, 6H, 15R, 21R, and 33R). The position of the signal corresponding to hhc stacking sequence, for convenience, is denoted as x_1 ppm. If

(33) Wyckoff, R. W. G. *Crystal structures*; Academic Press: New York, 1963; Vol. 1, pp 108−122.

Table 2. α Values and Existence Probabilities (*W*) Used in Figure 1B−1F

	continuing probability				existence probability			
	α_1	α_2	α_3	α_4	*W*(cc)	*W*(hc)	*W*(hh)	*W*(ch)
(A)	observed pattern							
(B)	0.90	0.80	0.20	0.80	0.71	0.10	0.09	0.10
(C)	0.90	0.20	0.80	0.80	0.47	0.23	0.07	0.23
(D)	0.20	0.80	0.80	0.80	0.30	0.30	0.10	0.30
(E)	0.90	0.20	0.80	0.20	0.40	0.20	0.20	0.20
(F)	0.90	0.80	0.80	0.20	0.71	0.10	0.09	0.10

ABCB(ch) is followed by an A layer with a probability α_4, we get ABCBA(chc) which corresponds to both 6H and 4H polytypes. This shows that a B site in the 6H polytype is the same environment as that in the 4H polytype. Further, the signals corresponding to the B site in 6H and 4H polytypes are very close, at −20.2 to −20.9 ppm[18,19,24,25] and −19.7 ppm,[25] respectively. If ABCB(ch) is followed by a C layer with a probability 1 − α_4, then the stacking sequence is ABCBC(chh) which also does not occur as a common polytype. The position of this signal is expressed as x_2. Table 1 summarizes eight kinds of the stacking modes for $R = 4$ and all of the signals in the NMR spectra.

The X-ray powder diffraction profiles of SiC were calculated using eq 7 in order to obtain α values to compare with the observed patterns. The X-ray powder diffraction pattern A in Figure 1 is the observed one of S-17. The calculated X-ray powder diffraction profiles (B−F) are obtained using the various values of α as shown in Figure 1. Profile B in Figure 1 shows the calculated profile based on $\alpha_1 = 0.90$, $\alpha_2 = 0.80$, $\alpha_3 = 0.20$, and $\alpha_4 = 0.80$. This profile does not correspond to the observed pattern because a broad peak, calculated at $2\theta = 38.0°$ (Cu Kα) and assigned as the (102) reflection of the 2H polytype, appears, which can't be accounted for in the observed pattern. In the calculated profile C (Figure 1), with $\alpha_1 = 0.90$, $\alpha_2 = 0.20$, $\alpha_3 = 0.80$, and $\alpha_4 = 0.80$, two additional peaks are calculated at $2\theta = 34.6°$ and $2\theta = 38.1°$ which correspond to the 4H polytype, which do not appear in the observed pattern. Figure 1D shows the calculated profile for $\alpha_1 = 0.20$, $\alpha_2 = 0.80$, $\alpha_3 = 0.80$, and $\alpha_4 = 0.80$. It can be noted that two peaks at $2\theta = 34.1°$ and $2\theta = 38.0°$, corresponding to the 6H polytype, do not appear in the observed pattern. The calculated profile for $\alpha_1 = 0.90$, $\alpha_2 = 0.20$, $\alpha_3 = 0.80$, and $\alpha_4 = 0.20$ is shown in Figure 1E. This calculated profile is not consistent with the observed pattern in view of the fact that the intensity of the reflection at $2\theta = 33.6°$ becomes very strong, and two weak broad peaks appear at $2\theta = 37.2°$ and $2\theta = 38.9°$. These two peaks are assigned to the new stacking mode because hhc and chh stacking sequences never appear as a common polytype as explained before. Figure 1F also shows the calculated profile for $\alpha_1 = 0.90$, $\alpha_2 = 0.80$, $\alpha_3 = 0.80$, and $\alpha_4 = 0.20$. The reflection at $2\theta = 60.1°$ becomes asymmetric, and it does not coincide with the observed pattern. All of the α values and calculated existence probabilities (*W*) for profiles B−F are summarized in Table 2. The α values are estimated on the basis of comparison of the calculated profiles (B−F) and the observed pattern in Figure 1. The final α values of S-17 are obtained when the reliability index (*R* factor) defined below becomes the smallest in the sequence of changing the α values at intervals of 0.01 step:

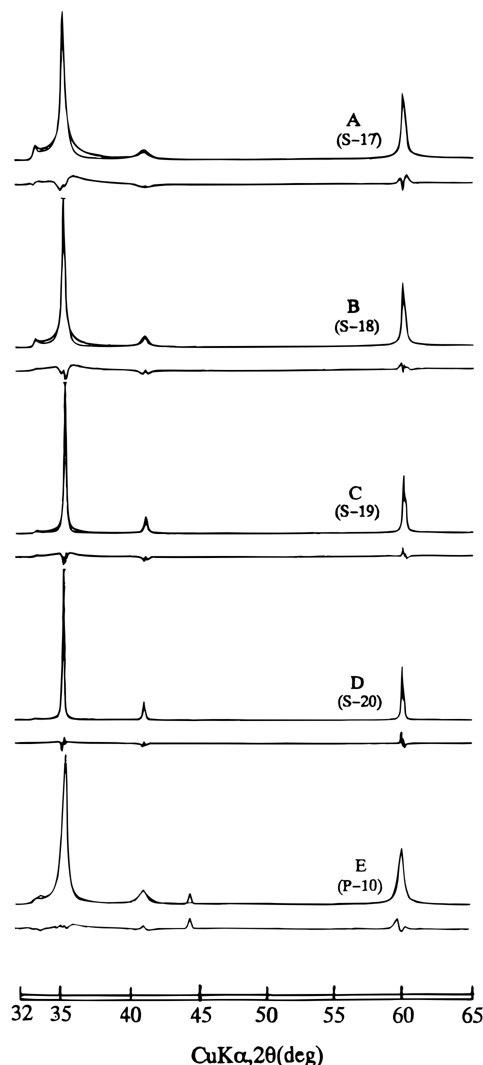

Figure 2. Observed patterns (—) and calculated profiles (···), and the differences between them of S-17, S-18, S-19, and S-20.

$$R = \sum[I_{T_{obs}}(2\theta) - I_{T_{calc}}(2\theta)]/\sum I_{T_{obs}}(2\theta)$$

where $I_{T_{obs}}$ is the observed intensity values and $I_{T_{calc}}$ is the calculated intensity values. The calculated α values are as follows: $\alpha_1 = 0.88$, $\alpha_2 = 0.76$, $\alpha_3 = 0.76$, and $\alpha_4 = 0.73$. Half-width and asymmetry parameters are at first obtained by the least-squares method, assuming that the sample does not include any stacking faults. The final *H* parameters obtained when the *R* factor becomes the smallest in the sequence of changing the *H* parameters at an interval of 0.001 are $H_1 = 0.009$, $H_2 = -0.005$, $H_3 = 0.007$, and $H_4 = 1.0$. The profile calculated using the final α values along with the observed pattern is shown in Figure 2A with the difference between the calculated profile and the observed pattern. As can be seen, there is a good agreement between the calculated profile and the observed pattern. The *R* factor is 0.16 and the calculated *W* values are *W*(cc) = 0.73, *W*(hc) = 0.12, *W*(hh) = 0.03 and *W*(ch) = 0.12. The X-ray powder diffraction profiles of the other three samples (S-18, S-19, and S-20) are calculated using the same method. The observed and calculated patterns and the differences between the calculated profiles and the observed patterns are shown in Figure 2B−D. The X-ray powder diffraction profile of plasma-produced SiC (P-10) is also calculated and

Table 3. α Values, *W* Values, *H* Parameters, and *R* Factor of Five Kinds of Synthetic SiC Calculated on the Basis of *R* = 4

Sample No.	α values				*W* values				*H* parameters				*R* factor
	α_1	α_2	α_3	α_4	*W*(cc)	*W*(hc)	*W*(hh)	*W*(ch)	H_1	H_2	H_3	H_4	*R*
A (S-17)	0.88	0.76	0.76	0.73	0.73	0.12	0.03	0.12	0.009	−0.005	0.007	1.0	0.17
B (S-18)	0.92	0.80	0.80	0.79	0.82	0.08	0.02	0.08	0.005	−0.002	0.003	1.0	0.16
C (S-19)	0.97	0.85	0.85	0.83	0.92	0.04	0.00	0.04	0.002	−0.0015	0.002	1.0	0.16
D (S-20)	0.98	0.88	0.88	0.88	0.96	0.02	0.00	0.02	0.001	−0.0010	0.001	1.0	0.17
E (P-10)	0.90	0.80	0.80	0.78	0.78	0.10	0.02	0.10	0.010	−0.005	0.009	1.0	0.19

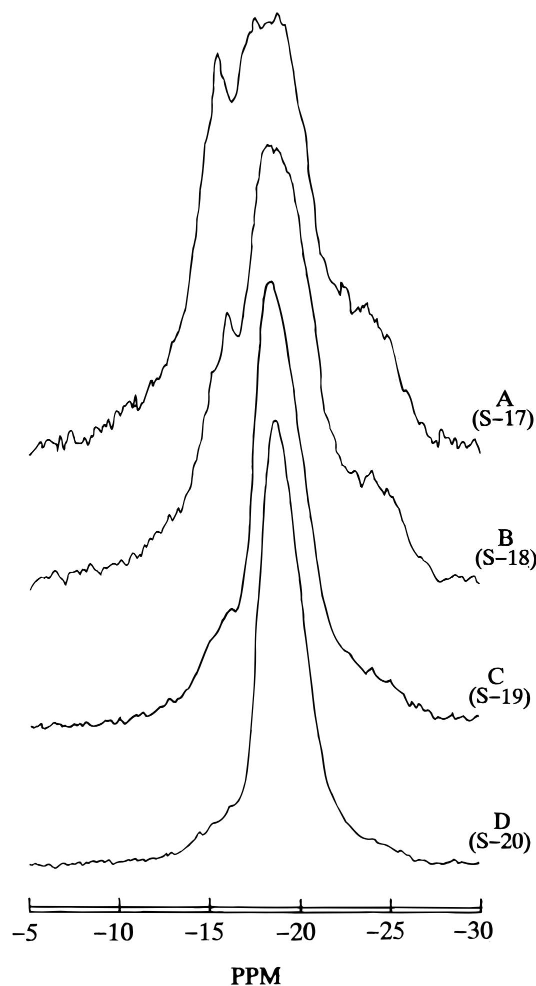

Figure 3. ^{29}Si MAS NMR spectra of S-17, S-18, S-19, and S-20.

compared with the observed pattern shown in Figure 2E. These results show that P-10 has a structure nearly similar to that of S-17 or S-18. The final α, *W*, *H*, and *R* values of all the samples are summarized in Table 3.

NMR Spectra of SiC with Stacking Faults. The NMR spectra of ^{29}Si obtained for the four samples (S-17, S-18, S-19, S-20) of SiC are shown in Figure 3. In the ^{29}Si NMR spectrum, Figure 3A, a broad peak is present at −18.5 ppm, along with a downfield signal at −16.1 ppm. A shoulder is also present at about −24.6 ppm. The line width (fwhh) of the major peak is about 6.6 ppm. In spectrum 3B, similar features are present as in the spectrum of 3A; however, the intensities of the downfield signal at −16.1 ppm and the shoulder at 24.6 ppm become weak. The line width of the major peak is about 5.6 ppm. Figure 3C shows the relatively narrower peak with a peak maximum at −18.5 ppm with a fwhh of 3.2 ppm, which has a shoulder on either side of the tall peak. In Figure 3D, the main peak occurs at −18.5 ppm with a fwhh of 2.6 ppm; however, a small shoulder

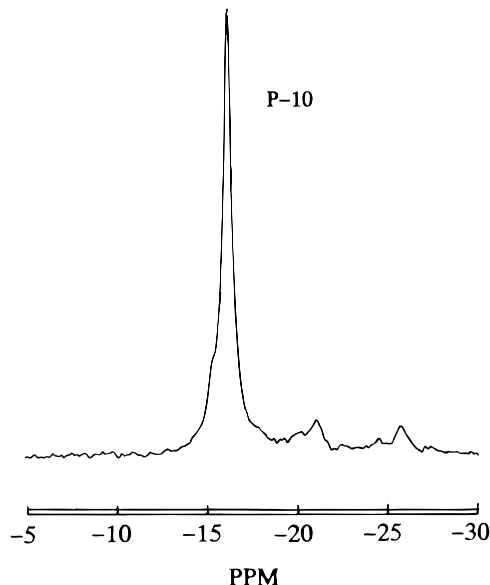

Figure 4. ^{29}Si MAS NMR spectrum of P-10.

at −16.1 ppm can be identified. With increasing synthesis temperature of the samples, the fwhh of the major peak at −18.5 ppm becomes narrower and the intensities of other signals at −16.1 and −24.6 ppm become weaker. In Figure 4, the ^{29}Si NMR spectrum of P-10 is shown. It consists of four signals at −15.2, −16.1, −20.5, and −24.8 ppm and has the narrowest fwhh (0.56 Hz) among the five samples.

The ^{29}Si NMR spectra of *β*-SiC samples have been reported.[17−19,23] The main discrepancy among these studies is that two main chemical shifts were reported; one is in the case of a plasma-produced SiC which shows a narrow single peak at around −16.3 ppm, and the other is in the case of SiC powder, produced by siliconizing porous carbon particles, which shows a broad peak at around −18.3 ppm. It is interesting to note that the NMR spectra of *β*-SiC show two different peaks despite the fact that *β*-SiC has only one crystallographically independent site. This ^{29}Si chemical shift at −16.3 ppm in *β*-SiC was called an anomalous peak.[17] The commercial *β*-SiC synthesized in an argon plasma has major ^{29}Si NMR chemical shifts at −16.3 ppm with minor upfield peaks which coincide with peaks of α-SiC. After heating this sample in an atmosphere of helium, all peaks including the anomalous peak disappear except the signal at −18.3 ppm.[17] Guth and Petusley[19] observed one sharp signal at −16.3 ppm in the case of a single crystal (particle size range 50−200 *μ*m). On the other hand, Wagner et al.[22] observed three different signals of similar *β*-SiC powders which were crushed in a hardened steel mortar. Carduner et al.[23] pointed out that the differences in these two cases are related to the formation of stacking faults in SiC powders. However, both the S-17 and P-10 samples have a similar

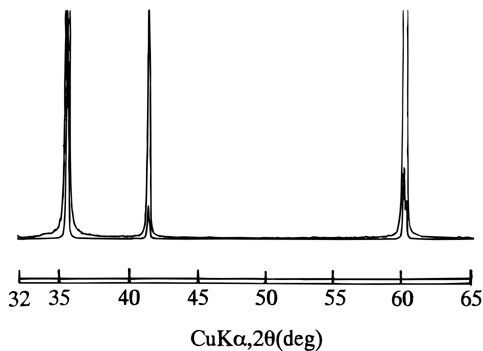

Figure 5. X-ray powder diffraction pattern of SiC sample annealed at 2000 °C.

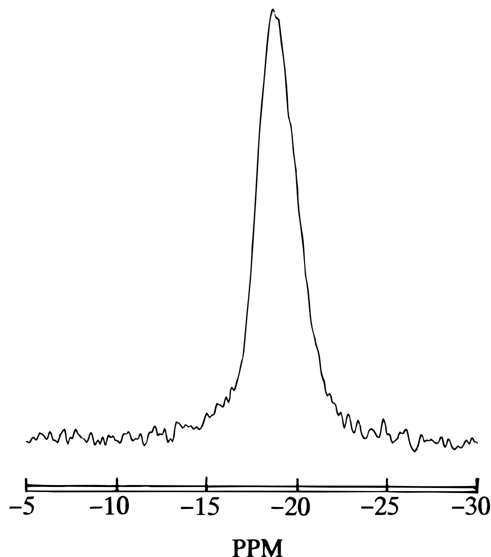

Figure 6. ^{29}Si MAS NMR spectrum of SiC sample annealed at 2000 °C.

amount of stacking faults in the structure in spite of the two samples showing completely different NMR spectra. Why the β-SiC sample shows two different major peaks still remains to be resolved. The sample of S-17 was therefore annealed at 2000 °C to remove the structural defects. The X-ray powder diffraction pattern of the annealed sample is shown in Figure 5. This pattern shows no peak at around $2\theta = 33.5°$, which indicates that this sample does not include any stacking faults in the structure. This annealed sample, therefore, is considered to be pure β-SiC without stacking faults. The ^{29}Si NMR spectrum of the annealed sample is shown in Figure 6. The main peak occurs at −18.5 ppm and the fwhh of the major peak is 2.6 ppm. This peak consists of one single signal, which indicates that the signal at −18.5 ppm should be assigned to pure β-SiC alone. However, pure β-SiC, which has one single narrow peak at −16.1 ppm, was also recently synthesized by laser-driven reactions and annealed at 1600 °C.[28,29] From a structural point of view, SiC produced by the present thermal decomposition method has almost the same structure as that of plasma- or laser-produced SiC; however, the ^{29}Si NMR spectra of the present SiC show very different patterns compared with that of plasma- or laser-produced SiC. These results indicate that the main difference in the ^{29}Si NMR spectra of the two samples may be caused by the small amount of paramagnetic impurities in the structure.

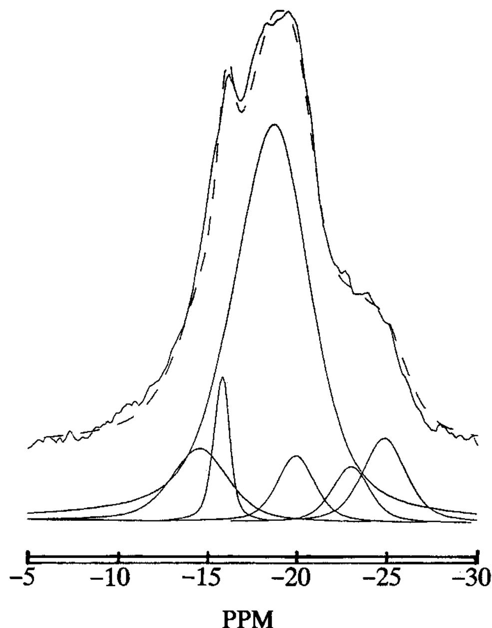

Figure 7. ^{29}Si MAS NMR spectrum of S-17 with the simulated results (- - -) using the six Gaussians.

It is possible to determine the relative amounts of stacking mode in each stacking sequence using spectral simulations and integrations of the ^{29}Si NMR spectra on the basis of the calculated X-ray powder diffraction profiles. The line-shape analysis was obtained using the Brucker visual curve-fitting program GLINFIT with a 3000 calculator. This program gives the position, width, relative intensity, area of each line, and rms percent error as a measure of the goodness-of-fit of the simulation. The largest discrepancy between simulation and experiment appears to be that the experimental lines are not exactly symmetrical but are generally skewed to the low ppm side. It is also somewhat difficult to analyze each component in the NMR spectra quantitatively because the NMR spectra are very sensitive to experimental conditions and the paramagnetic impurities, and there are some ambiguities (within 1 ppm) in the determination of the exact positions of all the signals.

Figure 7 shows the six deconvoluted Gaussian peaks, and their resultant simulated spectra are shown together with the recorded data for S-17. The relative simulated areas of each signal (S-17, S-18, S-19, S-20, and P-10) in Table 4 are close to the relative values calculated using the data for continuing and existence probability in Table 3 on the basis of the following formula, for example, $A_{3C} = W(cc)\alpha_1$, $A_{6H} = W(cc)(1 - \alpha_1)$. Both signals at around −16.1 and −18.5 ppm are considered to correspond to an A_{3C}-type signal. D_{X1}- and B_{X2}-type signals corresponding to hhc and chh stacking sequences were neglected to assign the chemical shifts because these associations do not appear in the usual polytype as explained before. However, if β-SiC forms from a 2H structure, which is stable at temperatures lower than 1300 °C,[34] these stacking modes may occur during the transition from the 2H to the 3C polytype. All of the samples show that the A_{3C}-type signal is the highest value among the six signals, and the $B_{4H,6H}$ and C_{6H}-type signals are high and almost the same values.

(34) Knippenberg, W. F. *Philips Res. Rep.* **1963**, 161.

Table 4. Relative Values of Each Stacking Mode Obtained from the Data for Calculated X-ray Diffraction Profile and Simulated NMR Spectra

symbol NMR (ppm)	A_{6H} −14.5 −15.2	A_{3C} −16.1 −18.4	D_{2H} $B_{4H,6H}$ −20.0 −20.5	C_{4H} −22.5	C_{6H} −24.5 −24.8	D_{X1} X_1	B_{X2} X_2
A (S-17) NMR	11	(6) 68 (62)	7	5	9		
XRD	9	65	(0) 9 (9)	3	9	2	3
B (S-18) NMR	8	(3) 78 (75)	5	3	6		
XRD	7	75	(0) 6 (6)	2	6	2	2
C (S-19) NMR	5	(2) 86 (84)	3	2	4		
XRD	3	89	(0) 3 (3)	0	3	0	1
D (S-20) NMR	2	(0) 94 (94)	1	1	2		
XRD	2	94	(0) 2 (2)	0	2	0	0
E (P-10) NMR	12	(76) 76 (0)	6	0	6		
XRD	8	70	(0) 8 (8)	2	8	2	2

If the α_1 value becomes small in keeping with the high α_2 and α_4 values as shown in Figure 1D, the polytype of the SiC changes from 3C to 6H. All of the present samples have high α_1, α_2, and α_4 values, which indicate that they include mainly the 3C and some amounts of the 6H stacking modes.

Conclusion

Submicron SiC powders commonly include stacking faults in their structure. The X-ray powder diffraction profiles of SiC including the stacking faults were calculated on the basis of "reichweite" $R = 4$ using the matrix intensity equation method. The number R denotes the correlation distance over which the occurrence of a layer type affects the probability of occurrence of a given layer. One-half of the X-ray diffraction correlation distance becomes 0.504 nm for $R = 4$, which nearly corresponds to the radius of the "sphere of influence" of 0.50 nm in the NMR spectra. The amount of stacking faults and the kinds of stacking modes among 2H, 3C, 4H, and 6H can, therefore, be discussed by comparing the calculated X-ray powder diffraction profiles and by the simulation of each deconvoluted signal in the NMR spectra. The relative simulated areas of six deconvoluted Gaussian peaks in the NMR spectra, which correspond to A_{3C}-, A_{6H}-, $B_{4H,6H}$-, C_{4H}-, C_{6H}-, and D_{2H}-type signals, were close to the relative amounts of six stacking modes, which correspond to the ccc, cch, chc, hch, hcc, and hhh in the Wyckoff notation, calculated using the data for continuing and existence probability obtained from the results of the simulated X-ray diffraction profiles. The simulated and calculated results indicate that all of the β-SiC samples used mainly consist of the 3C type and some amounts of the 6H stacking modes.

CM960471D